An Investigation on LTE Mobility Management

Ren-Huang Liou, Yi-Bing Lin, *Fellow*, *IEEE*, and Shang-Chih Tsai

Abstract—Mobility management in *Long Term Evolution* (LTE) is different from that in the third generation mobile telecom networks. In LTE, the *Mobility Management Entity* (MME) is responsible for the mobility management function. The MME is connected to a large number of evolved Node Bs (cells) that are grouped into the *Tracking Areas* (TAs). The TAs are further grouped into *TA Lists* (TALs). When a *User Equipment* (UE) moves out of the current TAL, it reports its new location to the MME. If the LTE network attempts to connect to the UE, the MME asks the cells in the TAL to page the UE. In LTE paging, the MME may sequentially page a cell, the TA of the cell, and/or the TAL of the cell. This paper investigates the performance of LTE paging, and provides the guidelines for the best paging sequence of cells.

Index Terms—Location update, long term evolution (LTE), mobility management, paging

1 Introduction

In a mobile telecom network, the locations of the *User Equipments* (UEs) are tracked so that incoming calls can be delivered to the UEs. Typical mobility management procedures include location update and paging. When a UE moves from one location to another location, the UE reports its new location to the network through the location update procedure. When an incoming call to the UE arrives, the network identifies the location of the UE via the paging procedure.

In *Long Term Evolution* (LTE), the *Mobility Management Entity* (MME; Fig. 1a) is responsible for the mobility management function [1], [2], which is connected to a group of *evolved Node Bs* (eNBs; the LTE term for base stations; see Fig. 1b). The radio coverage of an eNB (or a sector of the eNB) is called a cell (see the dashed squares; Fig. 1c). Every cell has a unique cell identity. The cells are grouped into the *Tracking Areas* (TAs; e.g., TA 1 contains Cell 1 and Cell 2 in Fig. 1d). Every TA has a unique *TA identity* (TAI). The TAs are further grouped into *TA Lists* (TALs) [1]. In Fig. 1, TAL 1 consists of TA 2, TA 3, and TA 4 (Fig. 1e).

A UE stores the TAL that includes the TA where the UE resides. In Fig. 1(1), the UE is covered by Cell 5, and the TAL it stores is TAL $1 = \{\mathrm{TA2}, \mathrm{TA3}, \mathrm{TA4}\}$. If the LTE network attempts to connect to the UE, it asks the cells in the TAL (e.g., Cell 3-Cell 8) to page the UE. Every eNB periodically broadcasts its TAI. The UE listens to the broadcast TAI and checks if the received TAI is in its TAL. If so, it means that the UE does not move out of the current location. In Fig. 1, when the UE moves from Cell 5 to Cell 7, it receives the TA 4 identity broadcast from eNB 7. Since TA 4 is included in TAL 1, the UE still resides in the same location. When the UE moves to Cell 9 (Fig. 1(2)), the received TA 5 identity (broadcast from eNB 9) is not found in TAL 1, which means that the UE has moved out of the current location. In this case, the UE executes the location update procedure to inform the MME that it has left TAL 1. The MME then assigns a new TAL to the UE. In Fig. 1, the new TAL is TAL $2 = \{\mathrm{TA4}, \mathrm{TA5}, \mathrm{TA6}\}$. Note that the TAL is assigned on a per-user basis (i.e., TALs for different UEs may have different sizes and shapes), and the newly assigned TAL may be overlapped with the previously assigned TAL (e.g., TAL 2 is overlapped with TAL 1 in Fig. 1). We consider the *central policy* [1] that assigns a new TAL whose central TA includes the cell where the UE currently resides. In Fig. 1(2), the UE resides in TA 5, and TAL $2 = \{\mathrm{TA4}, \mathrm{TA5}, \mathrm{TA6}\}$ is centered at TA 5. In the central policy, the TALs may be overlapped. For example, TA 4 is included in both TAL 1 and TAL 2.

When an incoming call to the UE arrives, it may incur large paging traffic if all cells in the TAL page the UE simultaneously. To resolve this issue, we implement three paging schemes in LTE. In this paper, an "interacted cell" refers to a cell where the UE is paged, makes calls, or performs location update. In other words, the interacted cell is the cell through which the UE had the interaction with the network.

- **Scheme CT (Cell-TAL).** When an incoming call arrives, the MME first asks the last interacted cell to page the UE. If fails, all cells in the TAL are asked to page the UE.
- **Scheme TT (TA-TAL).** When an incoming call arrives, the TA of the last interacted cell is asked to page the UE. If fails, all cells in the TAL are asked to page the UE.
- **Scheme CTT (Cell-TA-TAL).** When an incoming call arrives, the MME first asks the last interacted cell to page the UE. If fails, the TA of the last interacted cell is asked to page the UE. If fails again, all cells in the TAL are asked to page the UE.

- *R.-H. Liou and S.-C. Tsai are with the Department of Computer Science, National Chiao Tung University, No. 1001, University Road, Hsinchu City, Taiwan 300, R.O.C. E-mail: {rhliou, tsaisc}@cs.nctu.edu.tw.*
- *Y.-B. Lin is with the Department of Computer Science, National Chiao Tung University, No. 1001, University Road, Hsinchu City, Taiwan 300, R.O.C., the Institute of Information Science and the Research Center for Information Technology Innovation, Academia Sinica, Nankang, Taipei, Taiwan, R.O.C., and King Saud University. E-mail: liny@cs.nctu.edu.tw.*

Manuscript received 8 Aug. 2011; revised 2 Oct. 2011; accepted 11 Nov. 2011; published online 28 Nov. 2011.
For information on obtaining reprints of this article, please send e-mail to: tmc@computer.org, and reference IEEECS Log Number TMC-2011-08-0447. Digital Object Identifier no. 10.1109/TMC.2011.255.

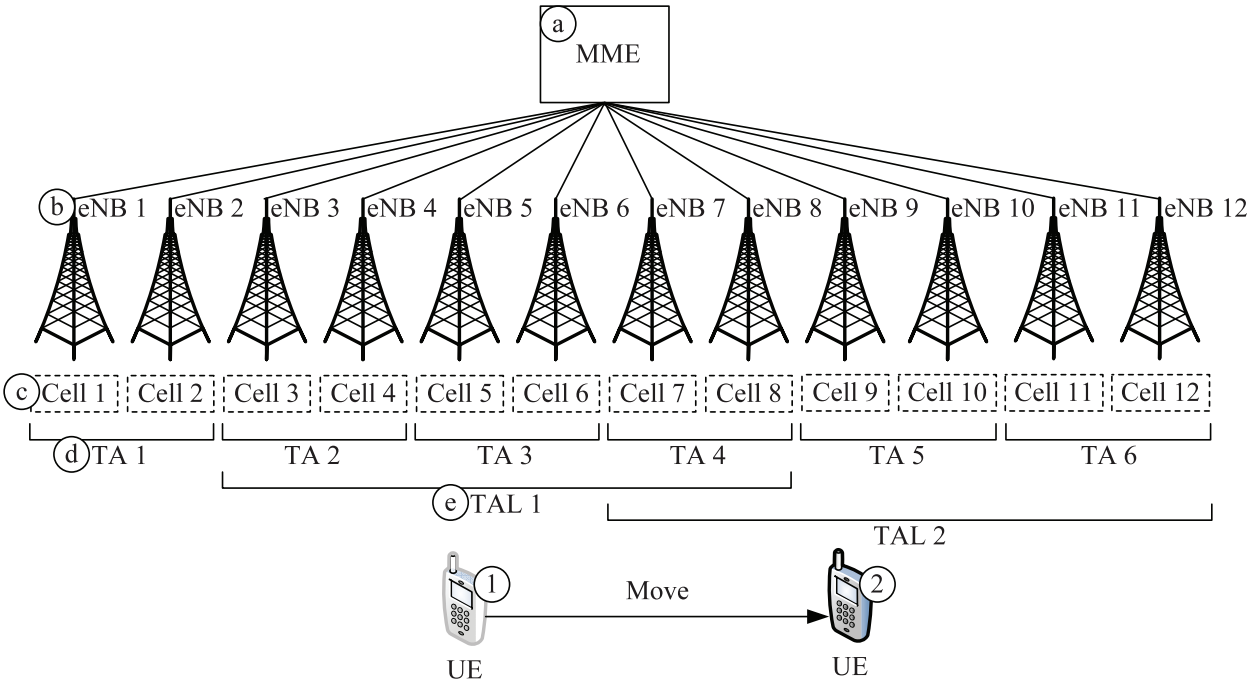

Fig. 1. LTE mobility management architecture.

Basically, the central policy and the three paging schemes we described for LTE mobility management partially implement the movement-based and the distance-based location updates [3], [4], [5] with the *Shortest-Distance-First* (SDF) paging [4], [6]. Although these schemes have been intensively studied in the literature, they have not been exercised in any commercial mobile telecom network because their implementations are not feasible. Specifically, in the distance-based location update, the UE is required to have the cell topology information (i.e., the distance relationship between cells) [3], [7], [8], which can not be practically implemented in a real network. In the SDF paging, it is difficult to dynamically define the neighboring cells (when the radio coverage changes, the "adjacent cells" may also change). Through the predefined TA configuration, LTE can partially implement the distance-based scheme with the SDF paging for commercial operation. In this paper, we show that LTE mobility management outperforms *third-generation* (3G) mobility management by capturing the advantages of the distance-based scheme with the SDF paging. We propose an analytic model to evaluate the performance of the TAL-based location update with the above three paging schemes.

This paper is organized as follows: Section 2 introduces the TAL-based location update. Section 3 proposes an analytic model for modeling the TAL-based scheme. Section 4 investigates the performance of the TAL-based scheme by numerical examples, and the conclusions are given in Section 5.

2 TAL-Based Location Update

This section describes the TAL-based location update by considering *one-dimensional* (1D) random walk model for the UE movement. This configuration significantly simplifies the description and provides better demonstration. Also, 1D configuration does exist in real environment [9]. We will extend the 1D model to a 2D model through simulation.

Fig. 2 illustrates the TAL configuration where a rectangular represents a cell. In this configuration, a TAL contains N_T TAs and each TA covers N_C cells. In a TAL, the TAs are sequentially labeled from 1 to N_T, and the cells are sequentially labeled from 1 to $N_C N_T$. To simplify our discussion on the central policy mentioned in Section 1, we assume that N_T is an odd number. Following the central policy, the TAL is overlapped with each of its adjacent TALs by $N_C\lfloor N_T/2\rfloor$ cells. Therefore, when the UE leaves the current TAL from Cell $N_C N_T$, the entrance cell of the newly assigned TAL is Cell $N_C\lfloor N_T/2\rfloor + 1$. Similarly, if the UE leaves the current TAL from Cell 1, the entrance cell of the newly assigned TAL is Cell $N_C(\lfloor N_T/2\rfloor + 1)$.

In most commercial 3G mobile telecom networks, the base stations are grouped into *Location Areas* (LAs) [10]. When the UE moves from old LA to new LA, a location update is performed. When an incoming call arrives, all cells in the LA of the UE will page the UE. The 3G mobility management scheme is a special case of the TAL-based location update with the TT paging where the size of an LA is the size of a TAL, and $N_T = 1$.

3 Analytic Modeling

This section models the TAL-based location update and the paging schemes. We first describe the input parameters and output measures.

Fig. 3 illustrates the timing diagram for the cell crossings and the incoming call arrivals. In this figure, we assume that the intercall arrival interval $t_c = \tau_2 - \tau_1$ is an exponential random variable with the mean $1/\lambda_c$. Let $t_{m,i} = t_{i+1} - t_i$ be the cell residence time between the $(i-1)$th cell crossing and the ith cell crossing. Assume that $t_{m,i}$ is independent

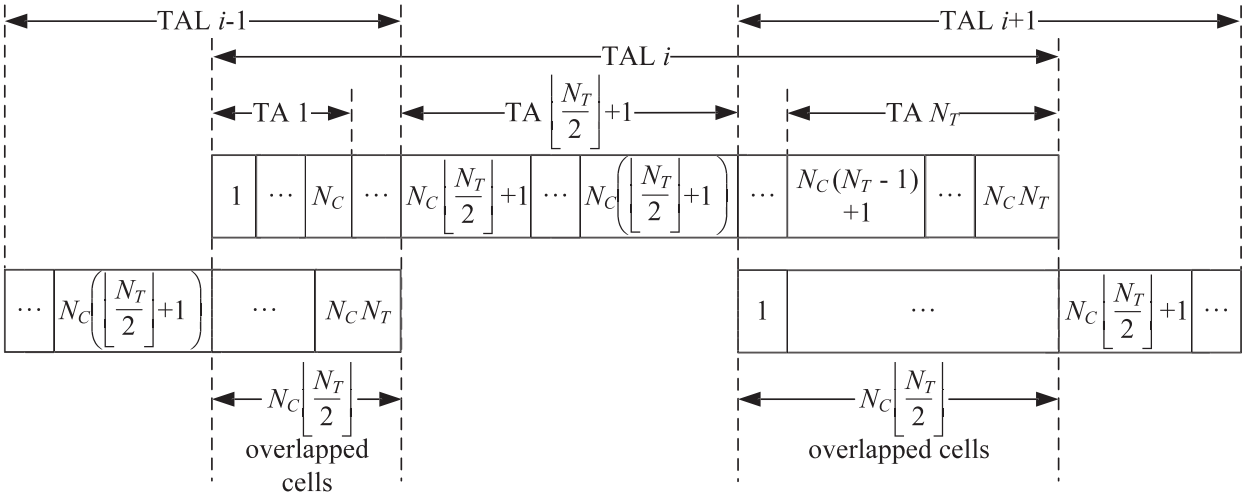

Fig. 2. The TAL configuration.

and identically distributed random variable with the mean $1/\lambda_m$, the variance V, and the Laplace transform $f_m^*(s)$. When the UE makes cell crossing, the UE moves to the right-hand side neighboring cell with routing probability p, and moves to the left-hand side neighboring cell with probability $1-p$. We consider the following three output measures:

- C_u: the expected number of location updates during t_c
- $C_{p,x}$: the expected number of cells that page the UE when an incoming call arrives, where $x \in \{CT, TT, CTT\}$
- $C_{d,x}$: the expected number of polling cycles [6] before the UE is found, where $x \in \{CT, TT, CTT\}$. Note that the maximum number of polling cycles for the CT, the TT, and the CTT schemes are 2, 2, and 3, respectively.

It is clear that the smaller the above output measures, the better the performance of the location update and paging schemes.

We first derive C_u. Let $E[M]$ be the expected number of cell crossings before the UE leaves the current TAL (i.e., the expected number of cell crossings between two consecutive location updates). Then, C_u can be computed as

$$C_u = \frac{E[t_c]}{E[M]E[t_{m,i}]} = \frac{\lambda_m}{\lambda_c E[M]}. \tag{1}$$

In [11], we have derived $E[M]$ with the following final formats. If $p = 0.5$,

$$E[M] = N_C\left(\left\lfloor \frac{N_T}{2} \right\rfloor + 1\right)\left(N_C\left\lfloor \frac{N_T}{2} \right\rfloor + 1\right). \tag{2}$$

If $p \neq 0.5$,

$$E[M] = \left\lceil \frac{A}{1+A-B} \right\rceil \left\lceil \frac{(N_C N_T + 1)B - N_C\lfloor \frac{N_T}{2} \rfloor - 1}{2p-1} \right\rceil + \left\lceil \frac{1-B}{1+A-B} \right\rceil \left\lceil \frac{(N_C N_T + 1)A - N_C(\lfloor \frac{N_T}{2} \rfloor + 1)}{2p-1} \right\rceil, \tag{3}$$

where

$$A = \frac{1-\left(\frac{1-p}{p}\right)^{N_C(\lfloor \frac{N_T}{2} \rfloor + 1)}}{1-\left(\frac{1-p}{p}\right)^{N_C N_T + 1}} \quad \text{and} \quad B = \frac{1-\left(\frac{1-p}{p}\right)^{N_C \lfloor \frac{N_T}{2} \rfloor + 1}}{1-\left(\frac{1-p}{p}\right)^{N_C N_T + 1}}. \tag{4}$$

Now we derive $C_{p,CT}$, $C_{p,TT}$, and $C_{p,CTT}$. Fig. 4 illustrates the state-transition diagram for the TAL-based location update. In this figure, state j represents that the UE resides in Cell j of the TAL, where $1 \le j \le N_C N_T$. For $2 \le j \le N_C N_T - 1$, the UE moves from state j to state $j+1$ with probability p, and moves from state j to state $j-1$ with probability $1-p$.

The state transition from state 1 to state $N_C(\lfloor N_T/2 \rfloor + 1)$ represents that the UE leaves the current TAL from Cell 1 and enters Cell $N_C(\lfloor N_T/2 \rfloor + 1)$ of the newly assigned TAL. Similarly, the transition from state $N_C N_T$ to state $N_C \lfloor N_T/2 \rfloor + 1$ represents that the UE leaves the current TAL from Cell $N_C N_T$ and enters Cell $N_C \lfloor N_T/2 \rfloor + 1$ of the newly assigned TAL. Let π_i be the steady-state probability that the UE resides in Cell i. From Fig. 4, we obtain the following balance equations:

$$\pi_i = \begin{cases} (1-p)\pi_{i+1}, & \text{for } i = 1 \\ p\pi_{i-1} + (1-p)\pi_{i+1}, & \text{for } 2 \le i \le N_C\left\lfloor \frac{N_T}{2} \right\rfloor, N_C\left\lfloor \frac{N_T}{2} \right\rfloor + 2 \le i \le N_C\left(\left\lfloor \frac{N_T}{2} \right\rfloor + 1\right) - 1 \text{ and } N_C\left(\left\lfloor \frac{N_T}{2} \right\rfloor + 1\right) + 1 \le i \le N_C N_T - 1 \\ p\pi_{i-1} + (1-p)\pi_{i+1} + p\pi_{N_C N_T}, & \text{for } i = N_C\lfloor \frac{N_T}{2} \rfloor + 1 \\ p\pi_{i-1} + (1-p)\pi_{i+1} + (1-p)\pi_1, & \text{for } i = N_C\left(\left\lfloor \frac{N_T}{2} \right\rfloor + 1\right) \\ p\pi_{i-1}, & \text{for } i = N_C N_T. \end{cases} \tag{5}$$

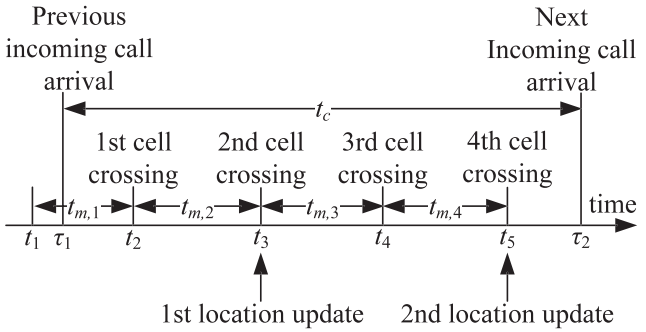

Fig. 3. Timing diagram for the cell crossings and the incoming call arrivals.

By rearranging (5), if $p = 0.5$, π_i can be rewritten as

$$\pi_i = \begin{cases} i\pi_1, & \text{for } 1 \le i \le N_c\left\lfloor \frac{N_T}{2} \right\rfloor + 1 \\ \left(N_C\left\lfloor \frac{N_T}{2} \right\rfloor + 1\right)\pi_1, & \text{for } N_c\left\lfloor \frac{N_T}{2} \right\rfloor + 1 < i \\ & \le N_c\left(\left\lfloor \frac{N_T}{2} \right\rfloor + 1\right) \\ \left(N_C N_T - i + 1\right)\pi_1, & \text{for } N_c\left(\left\lfloor \frac{N_T}{2} \right\rfloor + 1\right) < i \\ & \le N_C N_T. \end{cases} \quad (6)$$

If $p \neq 0.5$ and $N_T = 1$, π_i is rewritten as

$$\pi_i = \pi_1, \quad \text{for } 1 \le i \le N_C. \quad (7)$$

If $p \neq 0.5$ and $N_T \neq 1$, π_i is rewritten as

$$\pi_i = \begin{cases} \left(\frac{1}{1-p}\right)\left\{1 + \left(\frac{p^2}{2p-1}\right)\left[\left(\frac{p}{1-p}\right)^{i-2} - 1\right]\right\}\pi_1, \\ \qquad \text{for } 2 \le i \le N_C\left\lfloor \frac{N_T}{2} \right\rfloor + 1 \\ \left(\frac{1}{1-p}\right)\left\{1 + \left(\frac{p^2}{2p-1}\right)\left[\left(\frac{p}{1-p}\right)^{i-2} - 1\right]\right\}\pi_1 \\ -\left[\left(\frac{p}{1-p}\right)^{i-N_C\left\lfloor \frac{N_T}{2} \right\rfloor - 1} - 1\right]\left(\frac{p}{2p-1}\right)\pi_{N_C N_T}, \\ \qquad \text{for } N_C\left\lfloor \frac{N_T}{2} \right\rfloor + 1 < i \le N_C\left(\left\lfloor \frac{N_T}{2} \right\rfloor + 1\right) \\ \left\{1 + \left[\frac{(1-p)^2}{1-2p}\right]\left[\left(\frac{1-p}{p}\right)^{N_C N_T - i - 1} - 1\right]\right\} \times \left(\frac{\pi_{N_C N_T}}{p}\right), \\ \qquad \text{for } N_C\left(\left\lfloor \frac{N_T}{2} \right\rfloor + 1\right) \le i \le N_C N_T - 1, \end{cases} \quad (8)$$

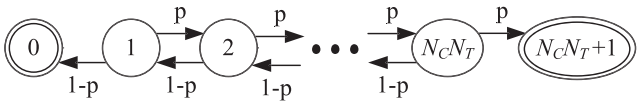

Fig. 5. State-transition diagram for 1D random walk model with two absorbing states.

and

$$\pi_{N_C N_T} = \left(\frac{1}{1-p}\right)\left\{1 + \left(\frac{p^2}{2p-1}\right)\left[\left(\frac{p}{1-p}\right)^{N_C\left\lfloor \frac{N_T}{2} \right\rfloor + N_C - 2} - 1\right]\right\} \left\{\left[\left(\frac{p}{1-p}\right)^{N_C - 1} - 1\right] \times \left(\frac{p}{2p-1}\right) + \frac{1}{p} + \left[\frac{(1-p)^2}{p(1-2p)}\right] \left[\left(\frac{1-p}{p}\right)^{N_C\left\lfloor \frac{N_T}{2} \right\rfloor - 1} - 1\right]\right\}^{-1} \pi_1. \quad (9)$$

Probability π_i can be solved by using $\sum_{i=1}^{N_C N_T} \pi_i = 1$ and (6)-(9).

Let $q_{i,j}^{(k)}$ be the probability that the UE moves from Cell i to Cell j after k cell crossings without any location update (it is possible that Cell j is revisited several times during these k cell crossings). Let $\bar{q}_{i,0}^{(k)}$ and $\bar{q}_{i,N_C N_T+1}^{(k)}$ be the probabilities that the UE initially stays in Cell i and moves out of the current TAL from Cell 1 and Cell $N_C N_T$ at the kth cell crossing, respectively. Probabilities $q_{i,j}^{(k)}$, $\bar{q}_{i,0}^{(k)}$, and $\bar{q}_{i,N_C N_T+1}^{(k)}$ are derived as follows. To compute the probability that the UE leaves the current TAL at the kth cell crossing (i.e., $\bar{q}_{i,0}^{(k)}$ and $\bar{q}_{i,N_C N_T+1}^{(k)}$), Fig. 5 modifies Fig. 4 by adding two absorbing states 0 and $N_C N_T + 1$ and removing the transitions from state 1 to state $N_C(\lfloor N_T/2 \rfloor + 1)$ and from $N_C N_T$ to $N_C\lfloor N_T/2 \rfloor + 1$. Let $q_{i,j}$ be the one-step transition probability from state i to state j. Fig. 5 illustrates the state-transition diagram, where the transition probability matrix $Q = (q_{i,j})$ of the random walk is

$$Q = \begin{pmatrix} 1 & 0 & 0 & 0 & \cdots & 0 & 0 & 0 \\ 1-p & 0 & p & 0 & \cdots & 0 & 0 & 0 \\ 0 & 1-p & 0 & p & \cdots & 0 & 0 & 0 \\ \vdots & \vdots & \vdots & \vdots & \ddots & \vdots & \vdots & \vdots \\ 0 & 0 & 0 & 0 & \cdots & 0 & p & 0 \\ 0 & 0 & 0 & 0 & \cdots & 1-p & 0 & p \\ 0 & 0 & 0 & 0 & \cdots & 0 & 0 & 1 \end{pmatrix}_{(N_C N_T+2)\times(N_C N_T+2).} \quad (10)$$

Let $Q^{(k)} = (q_{i,j}^{(k)})$ be the transition matrix. From (10), $Q^{(k)}$ is computed by the matrix multiplication $Q^{(k)} = \prod_{i=1}^{k} Q$. Based on $q_{i,j}^{(k)}$, $\bar{q}_{i,0}^{(k)}$ and $\bar{q}_{i,N_C N_T+1}^{(k)}$ are computed as

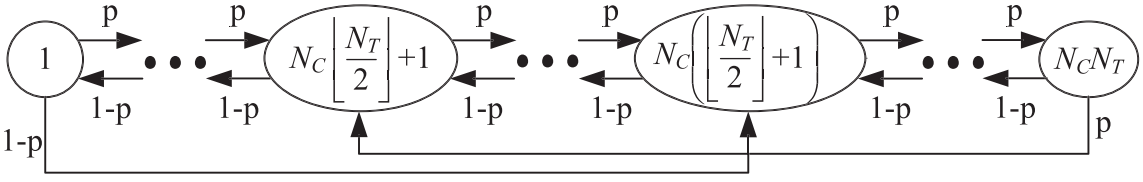

Fig. 4. State-transition diagram for TAL-based location update.

$$\bar{q}_{i,0}^{(k)} = \begin{cases} q_{i,0}, & \text{for } k = 1 \\ q_{i,0}^{(k)} - q_{i,0}^{(k-1)}, & \text{for } k > 1 \end{cases} \tag{11}$$

and

$$\bar{q}_{i,N_C N_T+1}^{(k)} = \begin{cases} q_{i,N_C N_T+1}, & \text{for } k = 1 \\ q_{i,N_C N_T+1}^{(k)} - q_{i,N_C N_T+1}^{(k-1)}, & \text{for } k > 1. \end{cases} \tag{12}$$

Given that the UE resides in Cell i when the previous incoming call arrives (i.e., Cell i is an "interacted cell"; see τ_1 in Fig. 3), let $\phi_i^{(k,n)}$ be the probability that after k cell crossings and n location updates, the UE moves back to the last interacted cell. If $n = 0$, then the last interacted cell is Cell i. If $n \geq 1$, the last interacted cell is the cell where the UE performs the nth location update. From (11) and (12), $\phi_i^{(k,n)}$ is computed as

$$\phi_i^{(k,n)} = \begin{cases} 1, & \text{for } k = 0 \text{ and } n = 0 \\ q_{i,i}^{(k)}, & \text{for } k > 0 \text{ and } n = 0 \\ \sum_{j=1}^{k} \Big\{ \phi_{N_C\left\lfloor \frac{N_T}{2} \right\rfloor+1}^{(k-j,n-1)} \bar{q}_{i,N_C N_T+1}^{(j)} & \\ \quad + \phi_{N_C\left(\left\lfloor \frac{N_T}{2} \right\rfloor+1\right)}^{(k-j,n-1)} \bar{q}_{i,0}^{(j)} \Big\}, & \text{for } k \geq n \geq 1 \\ 0, & \text{for } k < n. \end{cases} \tag{13}$$

In (13), for $k = 0$ and $n = 0$, the UE does not make any cell crossing (i.e., the UE still stays in Cell i), and $\phi_i^{(0,0)} = 1$. For $k > 0$ and $n = 0$, the last interacted cell is Cell i, and the probability that the UE moves from Cell i back to Cell i after k cell crossings without any location update is $q_{i,i}^{(k)}$. For $k \geq n \geq 1$, two cases are considered. First, if the UE moves out of the current TAL from Cell $N_C N_T$ at the jth cell crossing (with probability $\bar{q}_{i,N_C N_T+1}^{(j)}$), the last interacted cell is Cell $N_C\lfloor N_T/2 \rfloor + 1$ of the newly assigned TAL, and the numbers of the remaining cell crossings and location updates are $k - j$ and $n - 1$, respectively. Second, if the UE moves out of the current TAL from Cell 1 at the jth cell crossing (with probability $\bar{q}_{i,0}^{(j)}$), the last interacted cell is Cell $N_C(\lfloor N_T/2 \rfloor + 1)$ of the newly assigned TAL, and the numbers of the remaining cell crossings and location updates are $k - j$ and $n - 1$, respectively. For $k < n$, it is impossible that the number of cell crossings is smaller than that of location updates. Therefore, $\phi_i^{(k,n)} = 0$ for $k < n$.

Let $\beta(k)$ be the probability that the UE makes k cell crossings during t_c. From our previous work [6], $\beta(k)$ is derived as

$$\beta(k) = \begin{cases} 1 - \left(\frac{\lambda_m}{\lambda_c}\right)\left[1 - f_m^*(\lambda_c)\right], & \text{for } k = 0 \\ \left(\frac{\lambda_m}{\lambda_c}\right)\left[1 - f_m^*(\lambda_c)\right]^2 \left[f_m^*(\lambda_c)\right]^{k-1}, & \text{for } k > 0. \end{cases} \tag{14}$$

Assume that $t_{m,i}$ is a Gamma random variable with the mean $1/\lambda_m$, the variance V, and the Laplace transform

$$f_m^*(s) = \left(\frac{1}{V\lambda_m s + 1}\right)^{\frac{1}{V\lambda_m^2}}. \tag{15}$$

We consider the Gamma distribution because it has been shown that the distribution of any positive random variable can be approximated by a mixture of Gamma distributions [12]. The Gamma distribution was used to model UE movement in many studies [5], [6], [9] and is used in this paper to investigate the impact of variance for cell residence times. From (15), (14) is rewritten as

$$\beta(k) = \begin{cases} 1 - \left(\frac{\lambda_m}{\lambda_c}\right)\left[1 - \left(\frac{1}{V\lambda_m\lambda_c+1}\right)^{\frac{1}{V\lambda_m^2}}\right], & \text{for } k = 0 \\ \left(\frac{\lambda_m}{\lambda_c}\right)\left[1 - \left(\frac{1}{1V\lambda_m\lambda_c+1}\right)^{\frac{1}{V\lambda_m^2}}\right]^2 \left(\frac{1}{V\lambda_m\lambda_c+1}\right)^{\frac{k-1}{V\lambda_m^2}}, & \text{for } k > 0. \end{cases} \tag{16}$$

Let θ_C be the probability that the UE resides in the last interacted cell when an incoming call arrives. From (6)-(9), (13) and (16), θ_C is expressed as

$$\theta_C = \sum_{k=0}^{\infty} \beta(k) \sum_{i=1}^{N_C N_T} \pi_i \sum_{n=0}^{k} \phi_i^{(k,n)}. \tag{17}$$

In the right-hand side of (17), the UE makes k cell crossings during t_c with probability $\beta(k)$ ($0 \leq k \leq \infty$) and resides in Cell i with probability π_i ($1 \leq i \leq N_C N_T$) when the previous incoming call arrives. Therefore, θ_C is the summation of the product $\beta(k)\pi_i\phi_i^{(k,n)}$ over all possible (k, i, n) pairs (i.e., $0 \leq n \leq k \leq \infty$ and $1 \leq i \leq N_C N_T$).

Similar to $\phi_i^{(k,n)}$, let $\eta_i^{(k,n)}$ be the probability that after k cell crossings and n location updates, the UE moves back to the TA of the last interacted cell given that the UE resides in Cell i when the previous incoming call arrives. From (11) and (12), $\eta_i^{(k,n)}$ is derived as

$$\eta_i^{(k,n)} = \begin{cases} 1, & \text{for } k = 0 \text{ and } n = 0 \\ \sum_{j=N_C\left\lceil \frac{i}{N_C} \right\rceil - N_C+1}^{N_C\left\lceil \frac{i}{N_C} \right\rceil} q_{i,j}^{(k)}, & \text{for } k > 0 \text{ and } n = 0 \\ \sum_{j=1}^{k} \Big\{ \eta_{N_C\left\lfloor \frac{N_T}{2} \right\rfloor+1}^{(k-j,n-1)} \bar{q}_{i,N_C N_T+1}^{(j)} & \\ \quad + \eta_{N_C\left(\left\lfloor \frac{N_T}{2} \right\rfloor+1\right)}^{(k-j,n-1)} \bar{q}_{i,0}^{(j)} \Big\}, & \text{for } k \geq n \geq 1 \\ 0, & \text{for } k < n. \end{cases} \tag{18}$$

The explanation of (18) is similar to that of (13), and the details are omitted.

Let θ_T be the probability that the UE resides in the TA of the last interacted cell when an incoming call arrives. Similar to (17), from (6)-(9), (16) and (18), θ_T is expressed as

$$\theta_T = \sum_{k=0}^{\infty} \beta(k) \sum_{i=1}^{N_C N_T} \pi_i \sum_{n=0}^{k} \eta_i^{(k,n)}. \tag{19}$$

From (17) and (19), $C_{p,x}$ is computed as

$$C_{p,CT} = \theta_C + \big(1 - \theta_C\big)\big(1 + N_C N_T\big) \tag{20}$$

$$C_{p,TT} = \theta_T N_C + \big(1 - \theta_T\big)\big(N_C + N_C N_T\big), \tag{21}$$

and

$$C_{p,CTT} = \begin{cases} C_{p,CT}, & \text{for } N_C = 1 \\ \theta_C + (\theta_T - \theta_C)(1 + N_C) & \\ \quad + (1 - \theta_T)(1 + N_C + N_C N_T), & \text{for } N_C \neq 1. \end{cases} \tag{22}$$

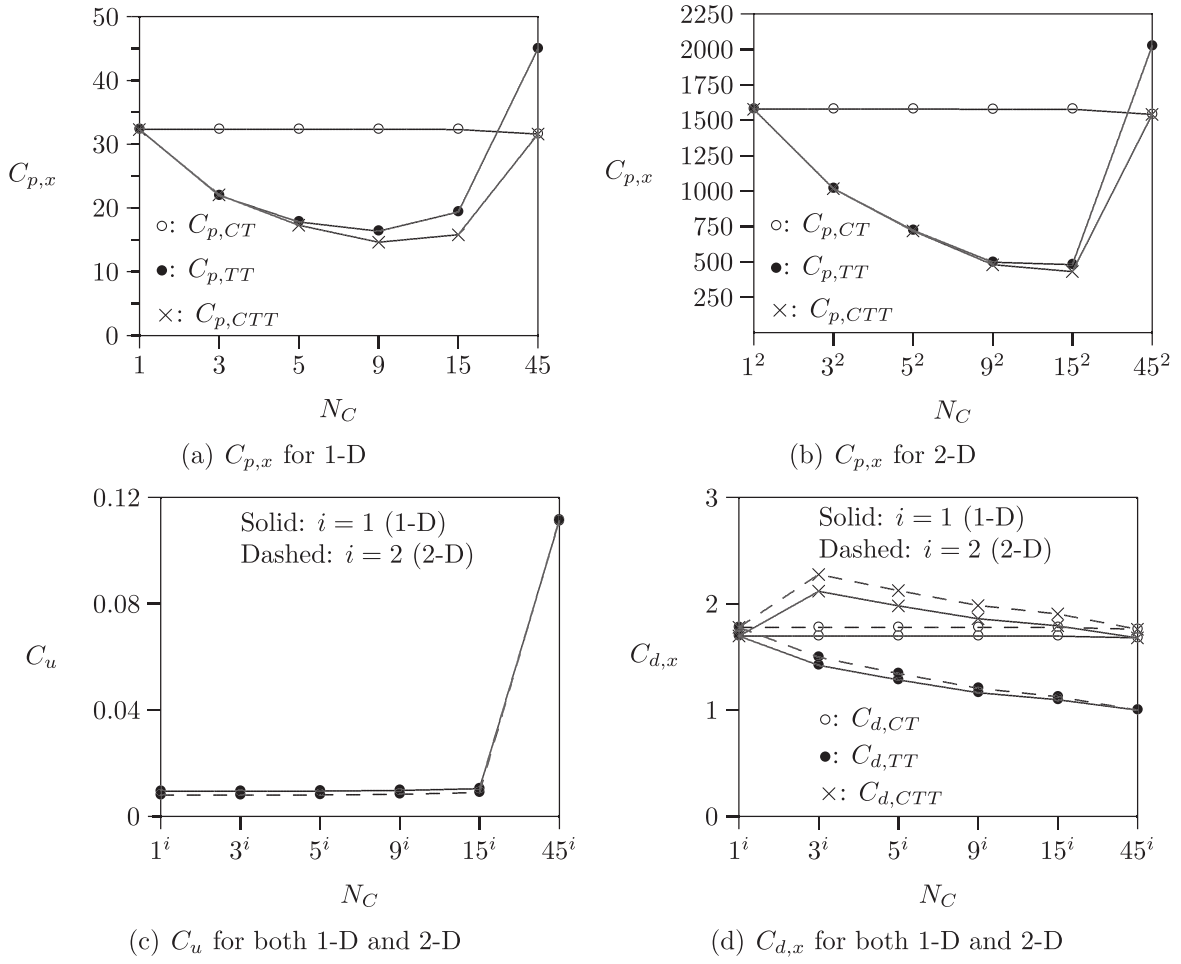

Fig. 6. Performance results for 1D ($p = 0.5$ and $N_C N_T = 45$) and 2D configurations ($p = 0.25$ and $N_C N_T = 45^2$), where $\lambda_m/\lambda_c = 5$ and $V = 1/\lambda_m^2$.

Similar to the derivations for $C_{p,x}$, $C_{d,x}$ is computed as

$$C_{d,CT} = \theta_C + 2(1 - \theta_C) = 2 - \theta_C, \tag{23}$$

$$C_{d,TT} = \theta_T + 2(1 - \theta_T) = 2 - \theta_T, \tag{24}$$

and

$$C_{d,CTT} = \begin{cases} C_{d,CT}, & \text{for } N_C = 1 \\ \theta_C + 2(\theta_T - \theta_C) + 3(1 - \theta_T), & \\ \quad = 3 - \theta_C - \theta_T, & \text{for } N_C \neq 1. \end{cases} \tag{25}$$

The major differences between our analytic model and the previous models for the movement-based and the distance-based schemes [5], [6] are described as follows:

- In the movement-based and the distance-based schemes, a location update or an incoming call resets the center cell of the residing area [6] to be the last interacted cell. On the other hand, the TAL-based location update resets the central TA of the TAL to be the TA of the last interacted cell (i.e., the last interacted cell may not be the center cell of the TAL). Therefore, our analytic model is more complicated than those for the movement-based and the distance-based location updates.
- In the SDF paging, the last interacted cell is the center cell of the subareas (i.e., the TA) [6]. In the TT and the CTT schemes, the last interacted cell may not be the center cell of the TA.
- The previous analytic models [5], [6] assume that the UE moves from a cell to one of the neighboring cells with the same probability. In our model, the UE can move to each of its neighboring cells with different probabilities.

Our analytic model is used to validate the discrete event simulation model (reviewers, please see the supplementary document, which can be found on the Computer Society Digital Library at http://doi.ieeecomputersociety.org/10.1109/TMC.2011.255). Simulation experiments show that the discrepancies between the analytic (i.e., (1), (20)-(25)) and simulation results are within 1 percent. After the simulation of 1D cell configuration has been validated by the analytic model, the validated simulation flowchart is extended to accommodate the 2D mesh cell configuration (i.e., Manhattan-street layout).

4 Numerical Examples

This section investigates the performance of the TAL-based location update and paging schemes. We first point out that the performance results for the 1D configuration are consistent with those for the 2D configuration. For $x \in \{CT, TT, CTT\}$, Fig. 6a plots $C_{p,x}$ for the 1D configuration,

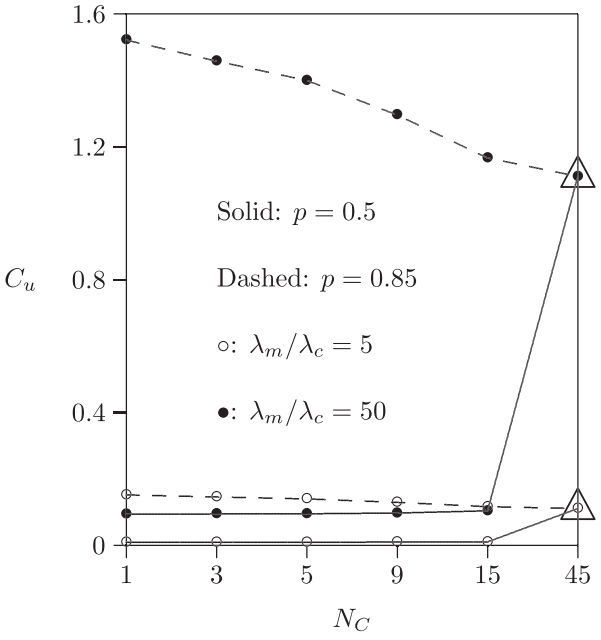

Fig. 7. Effects of p, λ_m/λ_c, and N_C on C_u ($N_C N_T = 45$).

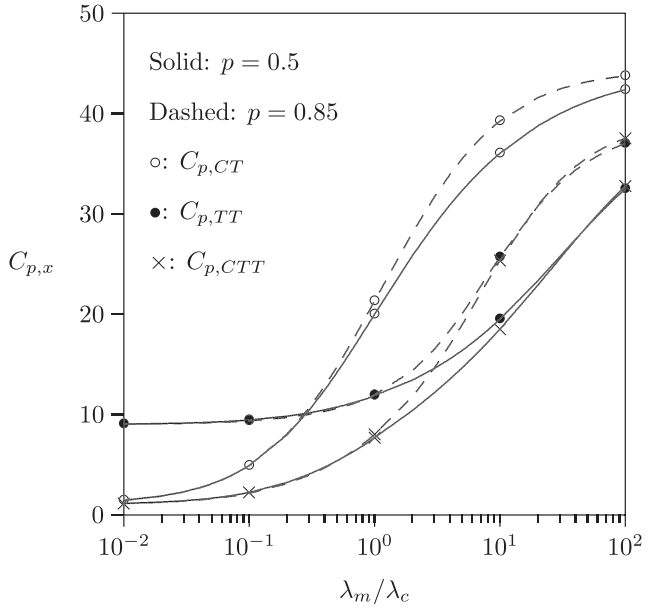

Fig. 8. Effects of λ_m/λ_c and p on $C_{p,x}$ ($N_C = 9$, $N_T = 5$ and $V = 1/\lambda_m^2$).

and Fig. 6b plots $C_{p,x}$ for the 2D configuration. Figs. 6c and 6d plot C_u and $C_{d,x}$ for both the 1D and the 2D configurations, respectively. In the 1D configuration, we consider the TAL size $N_C N_T = 45$ and $p = 0.5$. In the 2D mesh configuration, we consider a 45×45 cell structure, and the UE moves to one of the four neighboring cells with the same routing probabilities 0.25. This figure shows that the trends of $C_{p,x}$, C_u, and $C_{d,x}$ are similar for both the 1D and the 2D models. Therefore, our observations on the 1D model are also valid for the 2D model. For other input parameter setups, same results are observed, and the details are omitted.

The remainder of this section shows the results for the 1D configuration because several nontrivial observations can be easily explained through the analytic model of this simple configuration.

4.1 Analysis of the C_u Performance

In the 1D configuration, it suffices to consider $0.5 \leq p \leq 1$ in our study. In practice, a small p (e.g., $p = 0.5$; solid lines in Fig. 7) represents the movement of a pedestrian or a vehicle in local roads, which exhibits locality. A large p (e.g., $p = 0.85$; dashed lines in Fig. 7) represents the movement of a vehicle in highways. When p increases, the UE tends to move to one direction. Therefore, C_u increases as p increases. In Fig. 7, the values of the dashed curves ($p = 0.85$) are higher than those of the solid curves ($p = 0.5$).

When λ_m/λ_c increases (i.e., more cell crossings during t_c), more location updates are expected (i.e., C_u increases as λ_m/λ_c increases). In Fig. 7, the values of the • curves ($\lambda_m/\lambda_c = 50$) are higher than those of the ○ curves ($\lambda_m/\lambda_c = 5$).

The effect of N_C on C_u can be explained as follows. When $N_C = 1$, the entrance cell of the UE is the center cell of the new TAL. On the other hand, when $N_C = 45$ (i.e., $N_T = 1$ or the TAL only has one TA), the entrance cell of the UE is the boundary cell of the new TAL. Now consider $p = 0.5$. If $N_C = 1$, then it is unlikely that the UE will move out of the TAL in first few cell crossings. On the other hand, if $N_C = 45$, then the UE will move out of the TAL at the first cell crossing with probability 0.5. In other words, for a fixed $N_C N_T$ value, if p is small, $E[M]$ decreases as N_C increases. For example, for $N_C N_T = 45$ and $p = 0.5$, (2) indicates that $E[M] = 529$ for $N_C = 1$ and $E[M] = 45$ for $N_C = 45$. Since C_u is inversely proportional to $E[M]$ (see (1)), for a fixed $N_C N_T$ value, C_u increases as N_C increases for a small p (the solid curves in Fig. 7).

On the other hand, for a fixed $N_C N_T$ value, if p is large, $E[M]$ increases as N_C increases. In the extreme case, when $p = 1$, (3) is rewritten as $E[M] = N_C\lceil \frac{N_T}{2} \rceil$. If $N_C N_T = 45$, we have $E[M] = 23$ for $N_C = 1$ and $E[M] = 45$ for $N_C = 45$. Therefore, for a large p, C_u decreases as N_C increases (the dashed curves in Fig. 7).

As mentioned in Section 2, the 3G location update is a special case of the TAL-based scheme where $N_T = 1$ (i.e., $N_C = 45$; see the △ symbol in Fig. 7). When $p = 0.5$, the TAL-based scheme with $N_T \neq 1$ can reduce about 90 percent of the 3G location update cost. When $p = 0.85$, the TAL-based scheme with $N_T \neq 1$ incurs extra 4-36 percent cost over the 3G location update.

4.2 Analysis of the $C_{p,x}$ Performance

This section investigates the effects of λ_m/λ_c, p, V, and N_C on $C_{p,x}$.

- **Effects of** λ_m/λ_c: For all $x \in \{CT, TT, CTT\}$, Fig. 8 indicates that $C_{p,x}$ increase as λ_m/λ_c increases. When λ_m/λ_c increases, it is more likely that the UE is far away from the last interacted cell when an incoming call arrives, and thus higher $C_{p,x}$ are expected. When λ_m/λ_c is small, the low-mobility UE is more likely to be found in the last interacted cell, and there is no need to page the TA. In this case, we observe that $C_{p,CTT} < C_{p,CT} < C_{p,TT}$. On the other hand, when

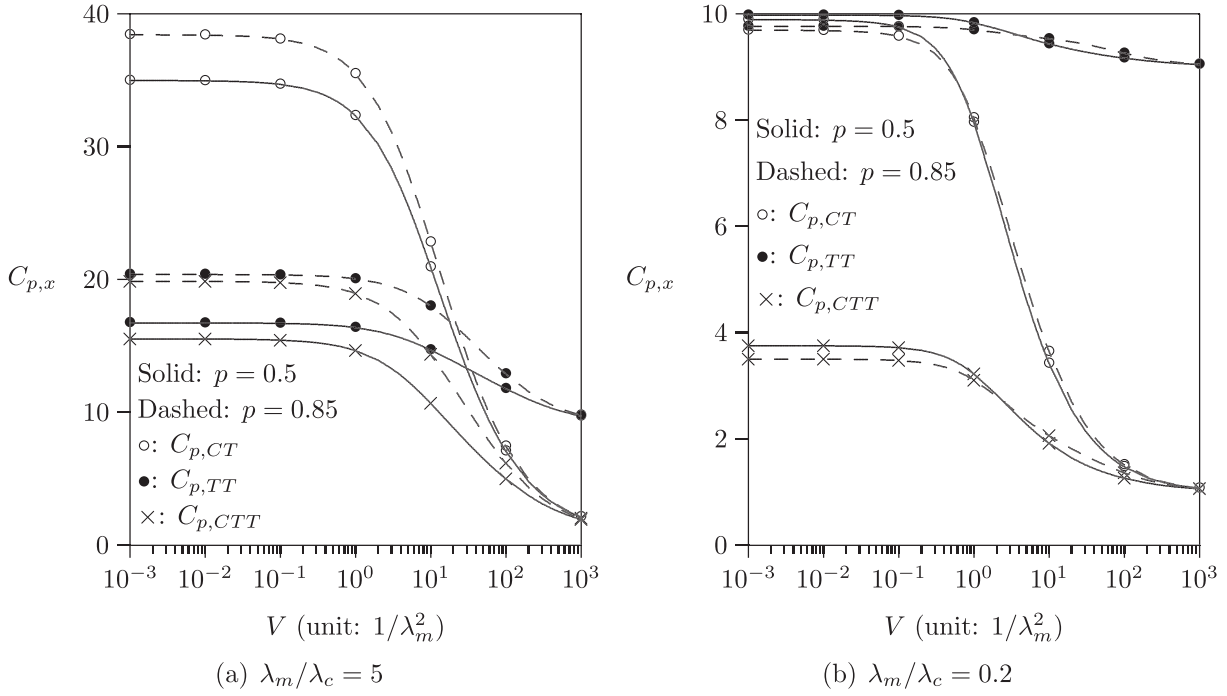

Fig. 9. Effects of V and p on $C_{p,x}$ ($N_C = 9$ and $N_T = 5$).

λ_m/λ_c is large, the UE is unlikely to reside in the last interacted cell, and paging the last interacted cell incurs extra paging cost. Therefore, $C_{p,CTT}$ is slightly larger than $C_{p,TT}$. The effect of λ_m/λ_c on $C_{p,CT}$ is more significant than that on $C_{p,CTT}$, and than that on $C_{p,TT}$. In summary, for small λ_m/λ_c, $C_{p,CTT} < C_{p,CT} < C_{p,TT}$. For large λ_m/λ_c, $C_{p,CTT} \approx C_{p,TT} < C_{p,CT}$.

- **Effects of** p: For all $x \in \{CT, TT, CTT\}$, Fig. 8 indicates that a large p incurs high paging costs $C_{p,x}$ because the UE may be far away from the last interacted cell when an incoming call arrives. The effect of p becomes more significant when λ_m/λ_c increases. Fig. 9 shows that the effects of p on $C_{p,x}$ become insignificant as V increases. In Figs. 8, 9, and 10, for most p values, $C_{p,CTT}$ are smaller than both $C_{p,CT}$ and $C_{p,TT}$.
- **Effects of** V: For a fixed λ_m value, we have the following facts about the variance V of the cell residence time $t_{m,i}$.
  - **Fact 1.** When V is small (i.e., the user movement pattern is regular), most $t_{m,i}$ have values around $1/\lambda_m$. In this case, if $\lambda_m/\lambda_c < 1$, the UE is likely to be found in the last interacted cell when an incoming call arrives. On the other hand, if $\lambda_m/\lambda_c > 1$, the UE is unlikely to be found in the last interacted cell.
  - **Fact 2.** For any λ_m value, when V increases (i.e., the user movement pattern becomes irregular), more longer $t_{m,i}$ periods will be observed, and the UE does not move in many consecutive t_c periods that fall in these $t_{m,i}$. In this case, the UE is always found in the last interacted cell, and lower $C_{p,x}$ are observed for all $x \in \{CT, TT, CTT\}$.

Due to Fact 1, when V is small and $\lambda_m/\lambda_c > 1$, the UE is unlikely to be found in the last interacted cell, and $C_{p,CT} > C_{p,TT}$ (in Fig. 9a, for $V \leq 1/\lambda_m^2$, the values of the ○ curves are higher than those of the ● curves). On the other hand, $C_{p,CT} < C_{p,TT}$ for a small λ_m/λ_c (in Fig. 9b, for $V \leq 1/\lambda_m^2$, the values of the ○ curves are lower than those of the ● curves). Due to Fact 2, Fig. 9 shows that when V is large, low $C_{p,x}$ are observed for all $x \in \{CT, TT, CTT\}$, and $C_{p,CT} < C_{p,TT}$. Specifically, when $V > 30/\lambda_m^2$, the values of the ○ curves are lower than those of the ● curves in Fig. 9a, and the values of the ○ curves are lower than those of the ● curves for all V values in Fig. 9b. The CTT scheme is a combination of the CT and the TT schemes, which explores the advantages of these two schemes in both large and small V scenarios, and yields the best performance. The effect of V on $C_{p,CT}$ is more significant than that on $C_{p,CTT}$, and than that on $C_{p,TT}$. In summary, when V is small, $C_{p,CTT} < C_{p,CT} < C_{p,TT}$ for a small λ_m/λ_c, and $C_{p,CTT} \approx C_{p,TT} < C_{p,CT}$ for a large λ_m/λ_c. When V is large, $C_{p,CTT} < C_{p,CT} < C_{p,TT}$.

- **Effects of** N_C: Since the CT scheme does not page the TA of the last interacted cell, $C_{p,CT}$ is not sensitive to the change of N_C (see the ○ curves in Fig. 10). Fig. 10a indicates that when V is small and $\lambda_m/\lambda_c > 1$, $C_{p,TT}$ decreases and then increases as N_C increases. In this case, the UE is unlikely to reside in the last interacted cell (Fact 1), and a large N_C results in a higher probability that the UE is found in the TA of the last interacted cell. Therefore, there is no need to page all cells in the TAL; i.e., lower $C_{p,TT}$ is observed. However, if N_C is "too" large, the cost of paging the TA is high, and the benefit of paging the TA becomes insignificant. Therefore, $C_{p,TT}$ decreases and then increases as N_C increases. Fig. 10b

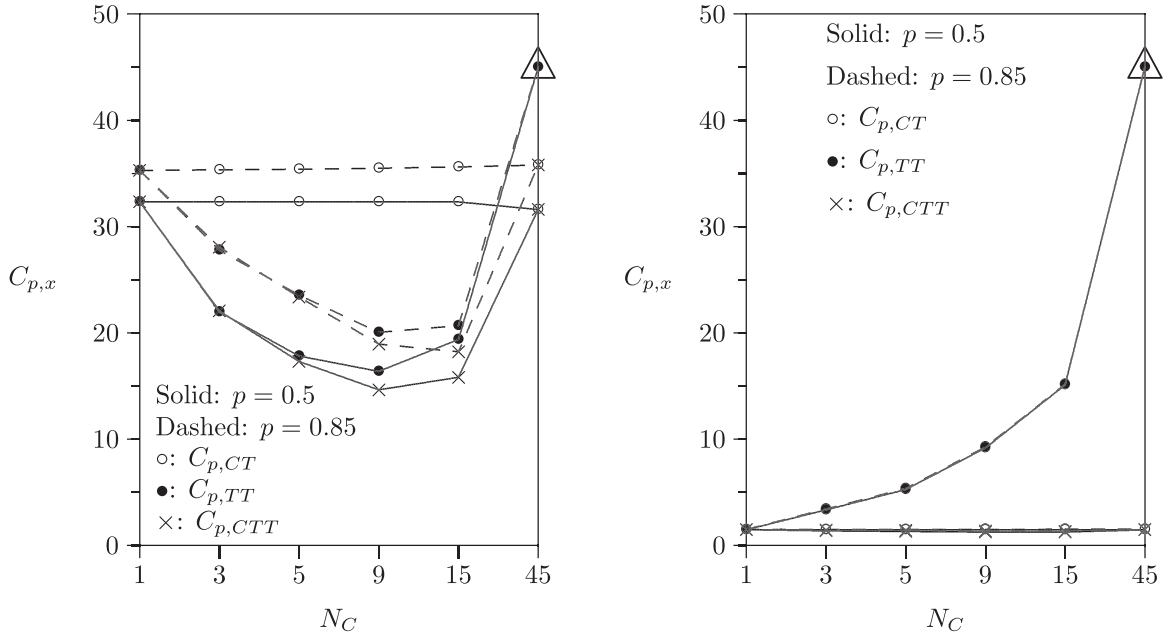

(a) $V = 1/\lambda_m^2$ and $\lambda_m/\lambda_c = 5$ (b) $V = 100/\lambda_m^2$ and $\lambda_m/\lambda_c = 0.2$

Fig. 10. Effects of N_C and p on $C_{p,x}$ ($N_C N_T = 45$).

indicates that when V is large and $\lambda_m/\lambda_c < 1$, $C_{p,TT}$ increases as N_C increases. In this case, the UE is more likely to be found in the last interacted cell (Fact 2), and it is a waste to page the TA (same result is observed for large V with $\lambda_m/\lambda_c > 1$). This extra cost becomes significant as the TA size is large (i.e., $C_{p,TT}$ increases as N_C increases). As we previously stated, the CTT scheme takes advantages of the CT and the TT schemes to yield the best performance for all N_C values. This figure also indicates that the lowest $C_{p,x}$ value can be found in the CTT scheme when $5 \leq N_C \leq 15$ (or $3 \leq N_T \leq 9$). Note that when $N_C = 1$, $C_{p,CT} = C_{p,TT} = C_{p,CTT}$ because a TA only contains one cell and paging the TA is the same as paging the cell (see (23)). On the other hand, when $N_C = 45$ (i.e., $N_T = 1$), a TAL only contains one TA, and $C_{p,CT} = C_{p,CTT}$.

As mentioned in Section 2, the 3G paging is a special case of the TT scheme where $N_T = 1$ (i.e., $N_C = 45$; see the $\triangle$ symbol in Fig. 10). Fig. 10 indicates that the TAL-based

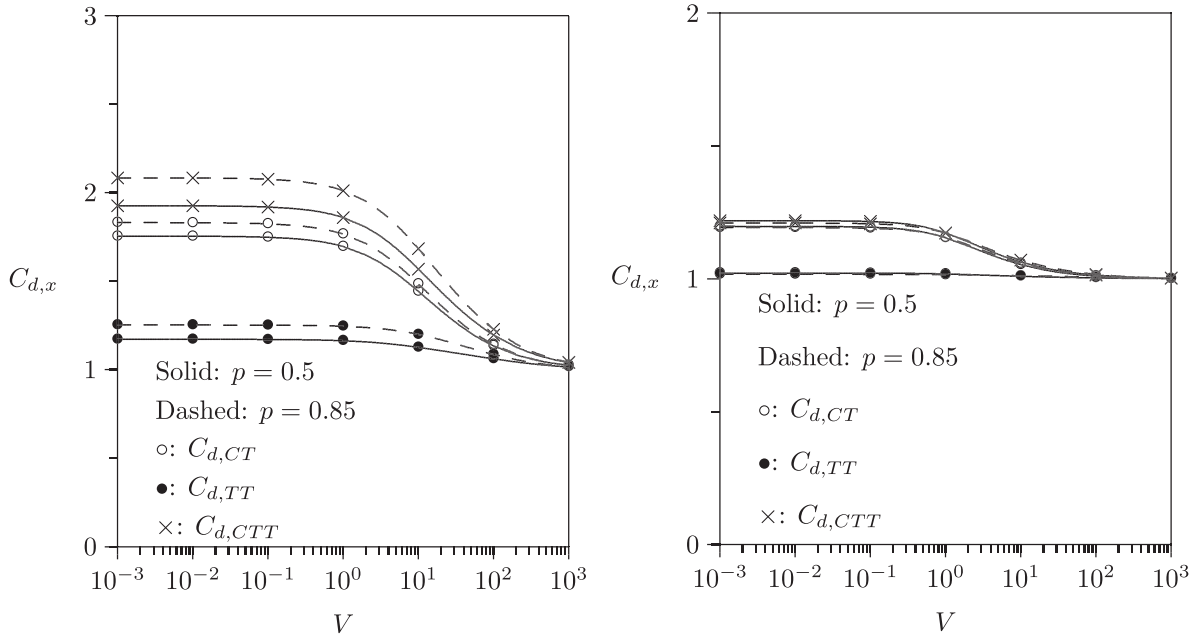

(a) $\lambda_m/\lambda_c = 5$ (b) $\lambda_m/\lambda_c = 0.2$

Fig. 11. Effects of λ_m/λ_c, p, and V on $C_{d,x}$ ($N_C = 9$ and $N_T = 5$).

paging schemes can reduce 21-97 percent of the 3G paging cost. For all input parameter setups under our study, the TAL-based paging schemes always outperform the 3G paging in terms of the $C_{p,x}$ performance.

4.3 Analysis of the $C_{d,x}$ Performance

Fig. 11 plots $C_{d,x}$ against λ_m/λ_c, p, and V. The effects of λ_m/λ_c, p, and V on $C_{d,x}$ are similar to those on $C_{p,x}$ described in Section 4.2, and the details are omitted. It is clear that $C_{d,TT} \leq C_{d,CT} \leq C_{d,CTT}$. As stated in Section 2, the 3G paging simultaneously asks all cells in the LA to page the UE, and thus the polling cycle is 1. The TAL-based paging schemes incur extra 0.01-1.08 polling cycles over the 3G paging for high mobility (Fig. 11a), and incur extra 0.01-0.21 polling cycle over the 3G paging for low mobility (Fig. 11b).

5 Conclusions

This paper investigated the performance of LTE mobility management. We considered the central policy for location update and three paging schemes based on the concept of TA and TAL. Our study indicates the following results:

- The central-based LTE location update outperforms the 3G location update by 90 percent for $p = 0.5$ (i.e., when the user movement exhibits locality). On the other hand, the LTE scheme incurs extra 4-36 percent cost over the 3G location update for $p = 0.85$ (i.e., when the user tends to move to one direction). We note that when $p \leq 0.75$, the TAL-based scheme always outperforms the 3G location update.
- The TAL-based paging schemes outperform the 3G paging by 21-97 percent in terms of the number of paged cells. Among the TAL-based paging schemes, the TT scheme outperforms the CT scheme when the variance V of the cell residence time is small (i.e., the user movement pattern is regular) and the UE moves frequently (i.e., λ_m/λ_c is large). The CT scheme outperforms the TT scheme when V is large or λ_m/λ_c is small. The CTT scheme takes advantages of both the CT and the TT schemes, which has the best performance in most input parameter setups under our study.
- For the number of polling cycles, the TAL-based paging schemes incur extra 0.01-1.08 polling cycles over the 3G paging. Among the TAL-based paging schemes, the TT scheme outperforms the CT and the CTT schemes.

In summary, if network signaling costs for location update and paging are major concern, then the CTT scheme should be selected. If the number of polling cycles is major concern, then the existing 3G mobility management should be selected for the users with high mobility and regular movement patterns (i.e., with small V). For low mobility users, the extra overheads incurred by the LTE paging can be ignored. Finally, the central-based LTE mobility management creates several interesting research issues. In the future, we will investigate the MME failure restoration based on dynamic TAL assignment [13], power saving [14], mobility management for mesh-mode LTE [15], handoff in heterogeneous network [16], and so on.

Acknowledgments

This work was supported in part by NSC 100-2221-E-009-070, Chunghwa Telecom, IBM, Arcadyan Technology Corporation, ICL/ITRI, Nokia Siemens Networks, and the MoE ATU plan.

References

[1] 3GPP, "General Packet Radio Service (GPRS) Enhancements for Evolved Universal Terrestrial Radio Access Network (E-UTRAN) Access," Technical Specification 3G TS 23.401, version 10.0.0 (2010-06), 2010.
[2] 3GPP, "Evolved Universal Terrestrial Radio Access (E-UTRA) and Evolved Universal Terrestrial Radio Access Network (E-UTRAN)," Technical Specification 3G TS 36.300, version 10.1.0 (2010-09), 2010.
[3] A. Bar-Noy, I. Kessler, and M. Sidi, "Mobile Users: to Update or Not to Update?" *Wireless Networks,* vol. 1, no. 2, pp. 175-185, 1995.
[4] J.S.M. Ho and I.F. Akyildiz, "Mobile User Location Update and Paging Under Delay Constraints," *Wireless Networks,* vol. 1, no. 4, pp. 413-425, 1995.
[5] R. Chen, S. Yuan, and J. Zhu, "A Dynamic Location Management Method of Personal Communication System," *Proc. E-Tech,* pp. 1-9, July 2004.
[6] I.F. Akyildiz, J.S.M. Ho, and Y.-B. Lin, "Movement-Based Location Update and Selective Paging for PCS Networks," *IEEE/ACM Trans. Networking,* vol. 4, no. 4, pp. 629-638, Aug. 1996.
[7] V.W.-S. Wong and V.C.M. Leung, "Location Management for Next-Generation Personal Communications Networks," *IEEE Network,* vol. 14, no. 5, pp. 18-24, Sept./Oct. 2000.
[8] I.F. Akyildiz, J. McNair, J.S.M. Ho, H. Uzunalioğlu, and W. Wang, "Mobility Management in Next-Generation Wireless Systems," *Proc. IEEE,* vol. 87, no. 8, pp. 1347-1384, Aug. 1999.
[9] Y.-B. Lin and Y.-C. Lin, "WiMAX Location Update for Vehicle Applications," *Mobile Networks and Applications,* vol. 15, no. 1, pp. 148-159, Feb. 2010.
[10] Y.-B. Lin and A.-C. Pang, *Wireless and Mobile All-IP Networks.* John Wiley & Sons., 2005.
[11] S.-R. Yang, Y.-C. Lin, and Y.-B. Lin, "Performance of Mobile Telecommunications Network with Overlapping Location Area Configuration," *IEEE Trans. Vehicular Technology,* vol. 57, no. 2, pp. 1285-1292, Mar. 2008.
[12] F.P. Kelly, *Reversibility and Stochastic Networks.* Wiley, 1979.
[13] Y.-B. Lin, "Per-User Checkpointing for Mobility Database Failure Restoration," *IEEE Trans. Mobile Computing,* vol. 4, no. 2, pp. 189-194, Mar./Apr. 2005.
[14] S.-R. Yang, S.-Y. Yan, and H.-N. Hung, "Modeling UMTS Power Saving with Bursty Packet Data Traffic," *IEEE Trans. Mobile Computing,* vol. 6, no. 12, pp. 1398-1409, Dec. 2007.
[15] D.-W. Huang, P. Lin, and C.-H. Gan, "Design and Performance Study for a Mobility Management Mechanism (WMM) Using Location Cache for Wireless Mesh Networks," *IEEE Trans. Mobile Computing,* vol. 7, no. 5, pp. 546-556, May 2008.
[16] N. Nasser, A. Hasswa, and H. Hassanein, "Handoffs in Fourth Generation Heterogeneous Networks," *IEEE Comm. Magazine,* vol. 44, no. 10, pp. 96-103, Oct. 2006.

Ren-Huang Liou received the BS and MS degrees in computer science from National Chiao Tung University (NCTU), Hsinchu, Taiwan, R.O.C., in 2007 and 2009, respectively. He is currently working toward the PhD degree at NCTU. His current research interests include Voice over Internet Protocol (VoIP), mobile computing, and performance modeling.

Yi-Bing Lin is a vice president and life chair professor in the College of Computer Science, National Chiao Tung University (NCTU), and a visiting professor of King Saud University. He is also with the Institute of Information Science and the Research Center for Information Technology Innovation, Academia Sinica, Nankang, Taipei, Taiwan, R.O.C. He is the author of the books *Wireless and Mobile Network Architecture* (Wiley, 2001), *Wireless and Mobile All-IP Networks* (John Wiley, 2005), and *Charging for Mobile All-IP Telecommunications* (Wiley, 2008). He has received numerous research awards including the 2005 NSC distinguished researcher award and the 2006 Academic Award of the Ministry of Education. He is a fellow of the IEEE, ACM, AAAS, and IET.

Shang-Chih Tsai received the BSCS degree from National Chiao Tung University (NCTU), Hsinchu, Taiwan, R.O.C., in 2008. He is currently working toward the MSCS degree at NCTU. His current research interests include design and analysis of a personal communications services network and performance modeling.